

Quasiclassical Theory of Spontaneous Currents at Surfaces and Interfaces of d -Wave Superconductors

M.H.S. Amin¹, A.N. Omelyanchouk², S.N. Rashkeev³, M. Coury¹, and A.M. Zagoskin^{1,4}

¹*D-Wave Systems Inc., 320-1985 West Broadway, Vancouver, B.C., V6J 4Y3, Canada;* ²*B.I. Verkin Institute for Low Temperature Physics and Engineering, Ukrainian National Academy of Sciences, Lenin Ave. 47, Kharkov 310164, Ukraine;*

³*Dept. of Physics and Astronomy, Vanderbilt University, Box 1807 Station B, Nashville, TN 37235, USA;* ⁴*Physics and Astronomy Dept., The University of British Columbia, 6224 Agricultural Rd., Vancouver, B.C., V6T 1Z1, Canada*

We investigate the properties of spontaneous currents generated at surfaces and interfaces of d -wave superconductors using the self-consistent quasiclassical Eilenberger equations. The influence of the roughness and reflectivity of the boundaries on the spontaneous current are studied. We show that these have very different effects at the surfaces compared to the interfaces, which reflects the different nature of the time reversal symmetry breaking states in these two systems. We find a signature of the “anomalous proximity effect” at rough d -wave interfaces. We also show that the existence of a subdominant order parameter, which is necessary for time reversal symmetry breaking at the surface, suppresses the spontaneous current generation due to proximity effect at the interface between two superconductors. We associate orbital moments to the spontaneous currents to explain the “superscreening” effect, which seems to be present at all ideal d -wave surfaces and interfaces, where d_{xy} is the favorite subdominant symmetry.

I. INTRODUCTION

The qualitative difference between d -wave and conventional (s -wave) superconductors is the intrinsic π -shift of the order parameter phase between the crystallographic a and b directions [1]. The most remarkable effects due to it are realized near surfaces and interfaces of such superconductors. In particular, depending on the direction of the crystalline axes on both sides of a Josephson junction, the equilibrium can be achieved not only at phase difference $\phi = 0$, like in conventional Josephson junctions, but at $\phi = \pi$ as well (“ π -junctions”) [1,2]. Therefore, a frustrated ring (a ring with an odd number of π -junctions) will have a time reversal symmetry breaking ground state, which supports a spontaneous magnetic flux $\pm\Phi_0/2$, where $\Phi_0 = \pi/e$ is the flux quantum (throughout this article we take $\hbar = k_B = 1$). Experiments [3–5] confirmed this prediction, thus establishing $d_{x^2-y^2}$ pairing symmetry of high- T_c cuprates.

The π -junctions are not specific to unconventional orbital symmetry (being first predicted [2] and recently realized [6] in SFS structures). They do not either provide the only way that \mathcal{T} -breaking states can appear in d -wave superconductors. We can distinguish between two situations: a doubly connected geometry, like a ring with π -junctions, and a simply connected one, like a single boundary between a d -wave superconductor and another differently oriented d -wave superconductor, s -wave superconductor, or vacuum. In the former case, the spontaneous flux is quantized (in units of $\Phi_0/2$) [1]. Therefore, the spontaneous currents are always present and flow through the whole ring (within the screening length from the surface which is, in high- T_c cuprates, of order 1500 Å). In the latter case, on the other hand, there is no quantization condition for the spontaneous flux and it can take arbitrary values [7,8]. The spontaneous currents

can be absent or confined to a much narrower area near the surface/interface itself, as we will see later.

A natural description of \mathcal{T} -breaking states near the surfaces and interfaces of d -wave superconductors can be given in the language of Andreev bound states [9]. They are formed by off-diagonal scattering of quasiparticles by a spatially inhomogeneous pairing potential, $\Delta(\mathbf{r})$. Off-diagonal means that the reflected quasiparticle changes the branch of the dispersion law (particle to hole and vice versa), so that electric charge $2e$ is being transferred to or from the condensate. Remarkably, Andreev reflection conserves spin (exactly) and momentum (with accuracy E/E_F , E being the quasiparticle energy measured from the Fermi level, E_F). As a result, the reflected hole is sent back with almost the same group velocity as the incident electron, and will therefore retrace its path (up to distance $\sim \xi_E = v_F/E$) in the clean limit (large elastic scattering length).

Mathematically, the Schrödinger equation for the (quasi-) electron wave function is now replaced by a matrix Bogoliubov–de Gennes equation [10] for two-component quasiparticle (bogolon) wave function $\Psi(\mathbf{r}) = \begin{pmatrix} u(\mathbf{r}) \\ v(\mathbf{r}) \end{pmatrix}$. The order parameter $\Delta(\mathbf{r})$ and its complex conjugate play the role of the off-diagonal components of the matrix scattering potential. If we neglect the self-consistency condition, which expresses $\Delta(\mathbf{r})$ through $u(\mathbf{r}), v(\mathbf{r})$, the equations are easily solved, and the positions of Andreev levels, E , are found from the Bohr-Sommerfeld quantization condition for a quasiclassical trajectory bounded by Andreev reflections at points L, R [10]:

$$\int_L^R p_{\text{elec}}(E)dl - \int_R^L p_{\text{hole}}(E)dl + \phi - \beta(E) = 2\pi n. \quad (1)$$

Here, the first and second terms represent the phase gain along the trajectory, ϕ is the phase difference between

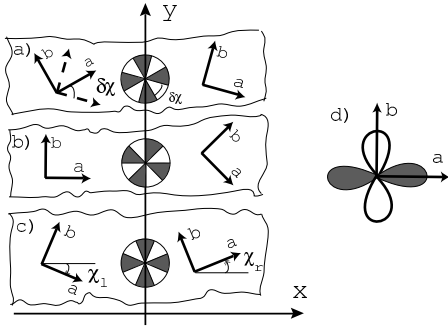


FIG. 1. Grain boundary junction between two d -wave superconductors. Here a and b denote the crystalline axes, and $\delta\chi$ is the mismatch angle. The y -axis is chosen along the grain boundary. The diagrams in the middle indicate the directions connecting the lobes of the order parameter with the same sign (shaded) and opposite sign, on both sides of the grain boundary. Supercurrent in the shaded directions is carried by regular Andreev levels, otherwise by π -levels (see text). For given $\delta\chi$, the properties of the junction depend on the grain boundary orientation vs. axes a, b . The special cases are asymmetric ($\chi_l = 0$) junction, (b), and symmetric junction, $\chi_l = -\chi_r$ (c). The positive and negative lobes of the order parameter are chosen along a and b respectively (d).

the order parameters in the points L, R (including the intrinsic phase difference), and the additional phase shift $\beta(E) = \pi \cdot O(1)$ depends on the shape of the scattering potential $\Delta(\mathbf{r})$ near the reflection points ($\beta(0) = \pi$). The minus sign before the second term reflects the quasiparticle branch change. Evidently, the right-moving electron and left-moving hole both carry electric current in the same direction. Therefore, unlike conventional standing wave solutions to the Schrödinger equation, Andreev bound states (Andreev levels) (Eq. (1)) carry electric current. This provides a mechanism for the Josephson effect in such structures as microbridges or in SNS contacts [11–13], which can be extended to the case of a general Josephson junction (see [14]). The current through a junction of unit width is expressed as [15]

$$I(\phi) = \frac{ek_F}{\pi} \sum_n \int_{-\pi/2}^{\pi/2} d\theta \cos\theta n_F[E_n(\phi, \theta)] \frac{dE_n(\phi, \theta)}{d\phi}.$$

Here, the x -axis is chosen normal to the grain boundary (see Fig. 1), $n_F(E)$ is the Fermi distribution function, and $E_n(\phi, \theta)$ is the energy of the n -th Andreev level for an electron with incidence angle θ . The direction-dependent intrinsic phase of Δ in d -wave superconductors leads to qualitatively new features of surface/interface states in d -wave superconductors (for current reviews see [16,17]). They stem from the coexistence of two types of Andreev levels, which are formed by Andreev reflections from the order parameter with the same (regular levels) or different (π -levels) intrinsic phases (see Fig. 1). In case of a d -wave superconductor boundary with an insulator, the

latter include so called midgap states (MGS), or zero energy states (ZES) [18], exactly at the Fermi level (since for $\phi = \pi$ the condition (1) is always satisfied by $E = 0$). The two sets of Andreev levels carry Josephson currents in opposite directions. In clean SND or DND junctions, as well as in short SD or DD point contacts, their contributions behave otherwise similarly. As a result, the current-phase dependence can become π -periodic [19–21]. What is more interesting, the equilibrium phase difference across such a junction is neither 0, nor π , but is degenerate, $\pm\phi_0$, which reflects the \mathcal{T} -breaking ground state of the system [7]. The value of ϕ_0 at $T = 0$ depends only on the orientation of the d -wave order parameter with respect to the boundary [21]. The occurrence of spontaneous currents in this picture is natural [7] (Fig. 2). In equilibrium, the Josephson current between the left and right superconductors (in the x -direction) is zero, which is possible only if the contributions of regular and π -levels cancel each other. But the y -components of these contributions add up, yielding a spontaneous current *along* the boundary. Evidently, there are two equilibrium states (with a spontaneous current flowing up or down).

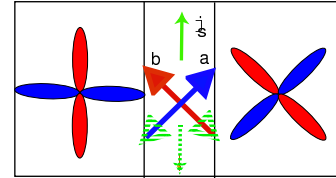


FIG. 2. Andreev levels and spontaneous currents in a DND model. The total superconducting current across the boundary, carried by normal levels (a) and π -levels (b), is zero in equilibrium, while the spontaneous current j_s parallel to the boundary is finite. The degeneracy of the ground state is illustrated by the freedom of choice of its direction.

This picture becomes more complicated in the presence of finite boundary transparency D , which breaks the symmetry between zero and π -states. The latter are not split by specular tunneling, and as a result, the amplitude of supercurrent carried by them scales as \sqrt{D} due to resonant transmission [15] (instead of D for regular levels). This led to the prediction of temperature-driven transition to π -junction [22] in a DD junction. Recent measurements of $I(\phi)$ in YBCO grain boundary junctions [23] generally confirmed this prediction, but showed that the transition does not necessarily occur between equilibrium values $\phi_0 = 0$ and $\phi_0 = \pi$.

Notice that in all of the above arguments we did not assume any subdominant order parameter. In other words, the \mathcal{T} -breaking and generation of the spontaneous current happens without any subdominant pairing potential. In general, a subdominant order parameter will occur at the boundary, if there exist interactions in the corresponding channel. In DD-junctions, the source of the subdominant order parameter is the proximity to a differ-

ently oriented superconductor and therefore it will exist at all temperatures even above the subdominant critical temperature T_{c2} . It is interesting that the presence of a subdominant interaction channel will actually suppress the spontaneous current [24]. We shall discuss this counterintuitive behavior in section III.

The role of the subdominant order parameter in the spontaneous current generation at surfaces is completely different. Near a boundary [e.g. the (110)-surface] the dominant $d_{x^2-y^2}$ order parameter is suppressed [25] and therefore a subdominant order parameter (d_{xy} or s) can appear. It will be formed below the smaller critical temperature T_{c2} if there exists nonzero pairing interaction in the corresponding channel [26]. The combination of the two order parameters with complex coefficients breaks the \mathcal{T} -symmetry [1] and can lead to spontaneous surface currents and magnetic fluxes. Usually $d_{x^2-y^2} \pm is$ or $d_{x^2-y^2} \pm id_{xy}$ combinations are predicted. Recent observations of zero bias peak splitting in surface tunneling experiments [27] and spontaneous fractional flux ($0.1-0.2 \Phi_0$) near the “green phase” inclusions in YBCO films [28] agree with this picture.

The simple description based on Andreev levels presented earlier is best suited for quasi-1D problems in SNS (or DND) structures. It is possible to generalize it to deal with at least some of the above mentioned complications [29,30] by introducing “Andreev tubes” of width $\sim \lambda_F$, following the quasiclassical trajectories. Nevertheless, in order to obtain quantitative results, it is better to use an approach based directly on the method of quasiclassical superconducting Green’s functions (Eilenberger equations [31]). In this paper we apply the formalism to the case of a planar d -wave superconductor in contact with another superconductor or vacuum, for an arbitrary transparency and roughness of the boundary.

The paper is organized as follows. In Section II, we consider the generation of spontaneous currents by the proximity effect at a uniform SD or DD interface. We obtain the equilibrium phase, the spontaneous current distribution, and the superscreening effect (in the latter case) in case of ideal, rough, and partly reflective surface. In Section III, the spontaneous current generated by the subdominant order parameter at a boundary is considered. The interplay of the two mechanisms (proximity effect and subdominant pairing) is discussed for DD and SD junctions. The technical details of the formalism are given in the appendices.

II. SPONTANEOUS CURRENT GENERATED BY PROXIMITY EFFECT

A. Ideal junctions

Let us consider a planar d -wave superconductor with a straight grain boundary along the y -axis in its ab -plane (cf. Fig. 1). The order parameter $\Delta(\mathbf{v}_F, \mathbf{r})$ is self-consistently determined by the interaction potential

$V(\mathbf{v}_F, \mathbf{v}'_F)$ [see Eq. (A4)]. In a pure $d_{x^2-y^2}$ case we assume the interaction potential to have the form

$$V(\mathbf{v}_F, \mathbf{v}'_F) = V_d \cos 2(\theta - \chi) \cos 2(\theta' - \chi), \quad (2)$$

where the angles θ, θ' give the direction of $\mathbf{v}_F, \mathbf{v}'_F$ in the ab -plane, and χ is the angle between the crystallographic a -direction and the x -axis. The dimensionless BCS constant of interaction is $\lambda_d = V_d N(0)/2$. We can also consider a boundary between a d -wave superconductor and an s -wave film in which case, for the s -wave superconductor, we have

$$V(\mathbf{v}_F, \mathbf{v}'_F) = V_s, \quad \lambda_s = V_s N(0). \quad (3)$$

This problem is essentially 1-dimensional, with $\Delta(\mathbf{v}_F, x) \rightarrow \Delta_{r,l}(\mathbf{v}_F)$ as $x \rightarrow \pm\infty$, where the subscripts l and r represent left and right of the boundary respectively. The method we choose to solve this problem is the standard quasiclassical method which is described in detail in appendix A. The self-consistent solution can be obtained only numerically (see appendix C). However, we start from the analytical solution in the simplest approximation, when we assume that the order parameter takes its bulk values at all x , there is no subdominant order parameter, and the grain boundary is ideal (transparent and specular, see appendix B).

We denote by $j_J [\equiv j_x(x=0)]$ the Josephson current flowing from the left to the right superconductor, and by $j_S [\equiv j_y(x=0)]$ the surface current flowing along the interface at the boundary. All the current distributions are expressed in units of j_c [defined in (A6)] which is of the order of the bulk critical current density. These currents are expressed by Eqs. (B8) and (B9) which are valid (within the applicability of the model) for arbitrary symmetry of the order parameters $\Delta_{l,r}$. For a DD interface, the functions $\Delta_{l,r}(\mathbf{v}_F)$ in (B8) and (B9) are

$$\Delta_{l,r} = \Delta_0(T) \cos 2(\theta - \chi_{l,r}), \quad (4)$$

where $\Delta_0(T)$ is the maximum gap, as introduced in appendix D. Note that in this section the pairing potential is assumed to be nonzero only in a single orbital channel on either side of the boundary. Therefore, while the anomalous Green’s functions (f, f^\dagger) which support *different* orbital symmetries are induced across the boundary, they do not translate into a subdominant order parameter Δ' .

The results of the calculations for a DD junction are displayed in Fig. 3 for different mismatch angles between the crystalline axes across the grain boundary and at temperature $T = 0.1T_c$ (assuming the same transition temperature on both sides). In all these figures, the left superconductor is assumed to be aligned with the boundary while the orientation of the right superconductor varies. The Josephson current-phase relation (Fig. 3a) demonstrates a continuous transition from a π -periodic (sawtooth-like) line-shape at $\delta\chi = 45^\circ$ to a 2π -periodic one for small $\delta\chi$, as expected in the case of a clean DND

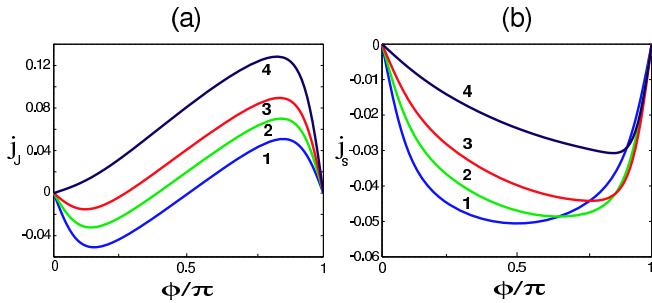


FIG. 3. Josephson current (a) and spontaneous current (b) versus the phase difference in a clean DD grain boundary junction calculated in non-self-consistent approximation. Current densities are in units of j_c [cf. Eq. (A6)] and $T = 0.1T_c$. The mismatch angles are $\chi_l = 0$ and $\chi_r = 45^\circ$ (1), 40° (2), 34° (3), 22.5° (4).

junction [21]. The phase dependence of the surface current (Fig. 3b) is also in qualitative agreement with earlier results for SND and DND junctions [7].

It is important to make a cautionary remark here. In order to have the Josephson effect, there must be a weak link between the two superconductors. In other words, the superconducting phase should change over a short distance at the boundary (otherwise one should speak about phase gradient and not phase difference). The weak link in a clean DND junction is provided by the normal layer, while in an ideal DD junction, it is formed due to the suppression of the order parameter near the boundary (at finite $\delta\chi$), which follows from self-consistent treatment. At $\delta\chi = 0$, such a “junction” (of infinite width) is simply a *bulk* superconductor and not a weak link, therefore Josephson physics does not apply. Nevertheless, the non-self-consistent approximation is applicable, in the limit $\delta\chi \rightarrow 0$, to the case of a narrow contact (microbridge) between the two sides, in a way similar to conventional superconductors [32].

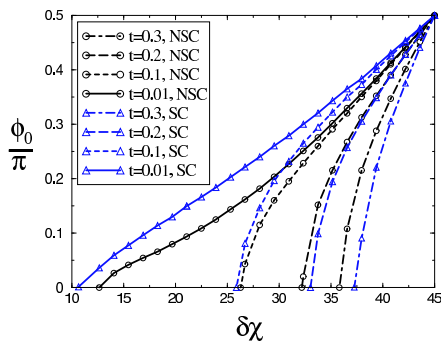


FIG. 4. Equilibrium phase difference in a clean DD grain boundary junction as a function of $\delta\chi \equiv \chi_r - \chi_l$ (keeping $\chi_l = 0$), at different values of $t \equiv T/T_c$. The circles and triangles correspond to non-self-consistent (NSC) and self-consistent (SC) calculations respectively. For nonzero ϕ_0 , the ground state is twice degenerate ($\phi = \pm\phi_0$).

The equilibrium phase difference across the junction, at which $j_J(\phi) = 0$ and $dj_J(\phi)/d\phi > 0$, takes any value between 0 and $\pi/2$, and is degenerate, $\phi = \pm\phi_0$, unless $\phi_0 = 0$. The \mathcal{T} -symmetry is therefore broken. The region of \mathcal{T} -breaking states (as a function of temperature and mismatch angle) is shown in Fig. 4. In that figure we also present the self-consistent numerical result for comparison. The method adopted for our numerical calculations is described in detail in appendix C. Only in the asymmetric $\delta\chi = 45^\circ$ junction does the degeneracy (at $\phi = \pm\pi/2$) survive at all temperatures, due to its special symmetry which leads to complete suppression of all odd harmonics of $I(\phi)$; generally, $\phi_0 \rightarrow 0$ at some temperature that depends on the orientation. The equilibrium value of the spontaneous current is nonzero in a certain region of angles and temperatures (Fig. 5), which is largest in the case of asymmetric $\delta\chi = 45^\circ$ junction.

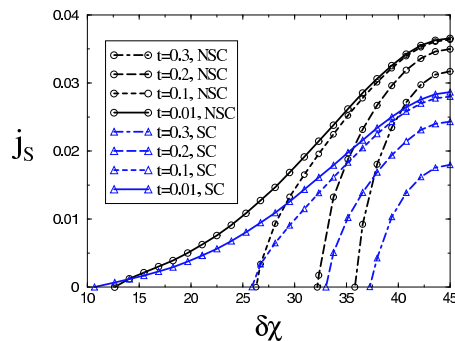


FIG. 5. Spontaneous current in the junction of Fig. 4.

We can also calculate the function $j_y(\mathbf{r})$ at all x using our analytical formalism [cf. Eq. (B10)]. This function is plotted in Fig. 6a. In this figure we also plot the same graph calculated using the self-consistent numerical method described in appendix C, with and without the subdominant order parameter (subdominant pairing is discussed in appendix D). The curves are qualitatively similar although there is a small quantitative difference. The same is true for the dominant order parameter, but not for the subdominant order parameter which appears only when the interaction in the corresponding channel exists (cf. Fig. 6b, Δ in this figure and all subsequent figures is normalized to T_c). Notice that the subdominant order parameter exists near the boundary despite $T > T_{c2}$. The reason is that the appearance of the subdominant order parameter is merely the result of the proximity effect, i.e., the extension of the order parameter from one region to the other, which happens at all temperatures.

In all of the graphs in Fig. 6a we see a remarkable feature: the current along the boundary is sharply peaked in a layer of order ξ_0 around it, but is accompanied by counterflows spread over about $10\xi_0$ on either side. Within the numerical accuracy, the total current in y -direction is *zero*, independently on either side of the junction.

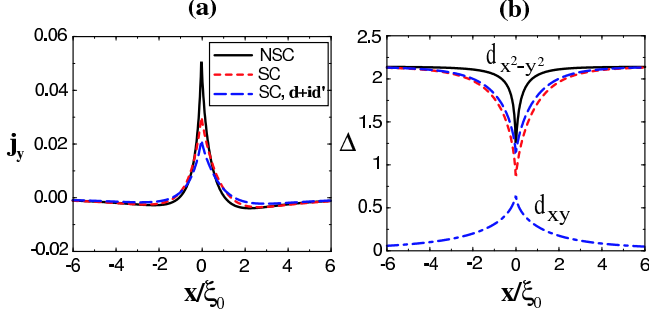


FIG. 6. Equilibrium spontaneous current distribution (a) and order parameter (b) for a (0° - 45°) grain boundary junction at $t = 0.1$. Solid and dashed lines represent the results of non-self-consistent and self-consistent calculations respectively. Long-dashed and dot-dashed lines represent the case with interaction in the subdominant d_{xy} channel ($t_{c2} \equiv T_{c2}/T_c = 0.05$).

Since in high- T_c superconductors $10\xi_0 \ll \lambda_L, \lambda_J$ (London and Josephson penetration depth respectively), the phenomenon can be called *superscreening* [24]. Note that we so far did not take into account the Meissner screening – and as it turns out don’t need to; the magnetic field of spontaneous currents is cancelled on a scale less than λ_L . This effect may be responsible for difficulties with observing spontaneous currents at surfaces and interfaces of d -wave superconductors [33], although as we will see, the effect is suppressed by roughness or reflectivity of the boundary.

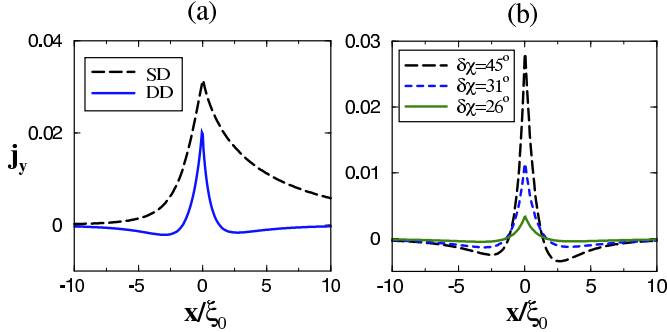


FIG. 7. (a) Spatial distribution of spontaneous current density in SD and asymmetric DD clean junctions at $t = t_{c2} = 0.05$ and $t_{cs} = 0.1$. In both cases $\chi_l = 45^\circ$ and in the DD case $\chi_r = 0$. (b) Spontaneous current near DD junctions with different misorientation angles $\chi_l = 0$ and $\chi_r = \delta\chi$ at $t = 0.1$. Calculations in this figure and in all subsequent figures are done self-consistently.

In the case $\delta\chi = 45^\circ$, the superscreening can be obtained analytically from Eq. (B10); the integral

$$\int_0^{\pm\infty} dx j_y(x) \propto \quad (5)$$

$$T \sum_{\omega > 0} \left\langle \frac{\Delta_l \Delta_r \sin \theta \operatorname{sign}(\cos \theta) \sin \phi}{\Omega_l \Omega_r + \omega^2 + \Delta_l \Delta_r \cos \phi} \cdot \frac{|v_F \cos \theta|}{\Omega_r} \right\rangle_\theta$$

is exactly zero after angular averaging. However, self-consistent numerical calculations show (within the numerical accuracy) the same behavior at all orientations (Fig. 7b). To better understand the situation, let us recall that in a system with local magnetic moment density $\mathbf{m}(\mathbf{r})$ the “molecular currents” flow with density $\mathbf{j}(\mathbf{r}) = c\nabla \times \mathbf{m}(\mathbf{r})$ (Fig. 8). In a superconductor with order parameter $d_{x^2-y^2} + e^{i\phi_0} d_{xy}$, the local orbital/magnetic moment density is

$$\begin{aligned} \mathbf{l}(\mathbf{r}) &\propto \mathbf{m}(\mathbf{r}) \propto \hat{\mathbf{z}} \int_0^{2\pi} \frac{d\theta}{2\pi} (\Delta_1(x) \cos 2\theta + \Delta_2(x) e^{-i\phi_0} \sin 2\theta) \\ &\times \frac{1}{i} \frac{\partial}{\partial \theta} (\Delta_1(x) \cos 2\theta + \Delta_2(x) e^{i\phi_0} \sin 2\theta) \\ &= 2\Delta_1(x)\Delta_2(x)\hat{\mathbf{z}} \sin \phi_0. \end{aligned}$$

The contribution to the spontaneous current is thus $\mathbf{j}(\mathbf{r}) \propto \nabla \times \mathbf{l}(\mathbf{r}) \parallel \hat{\mathbf{y}}$. Note that the same expression is obtained from the Ginzburg–Landau equations [34]: $\mathbf{j} \propto \nabla \times \hat{\mathbf{z}} \operatorname{Im}[d_1(\mathbf{r}) d_2^*(\mathbf{r})]$. The total current in the y -direction due to this mechanism is $I_{tot} \propto \int_\Omega d\mathbf{S} \cdot \nabla \times \mathbf{m} \propto \oint_{\partial\Omega} d\mathbf{s} \cdot \mathbf{m}$, where Ω is a cross-section in the xz -plane (assuming the superconducting film has finite thickness h), and $d\mathbf{s}$ is the linear element of its boundary $\partial\Omega$. The latter integral is obviously zero, because either $\mathbf{m} \parallel \hat{\mathbf{z}} \perp d\mathbf{s}$ (when $z = \pm h/2$), or $\mathbf{m} = 0$ (at $x = \pm\infty$, where the contour $\partial\Omega$ is closed). Moreover, the “molecular currents” picture, shown in Fig. 8, reproduces to the distinct peak-and-counterflow current distribution.

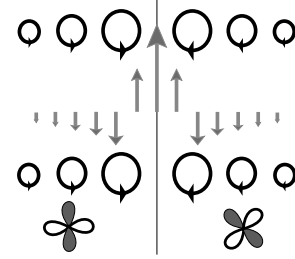


FIG. 8. “Molecular currents”: the supercurrent distribution in a DD junction as the superposition of local currents produced by the angular momenta of Cooper pairs in a chiral $d + e^{\pm i\phi_0} d'$ state.

A finite magnetic moment in the bulk is essential for the effect. The corresponding chiral state is created by the proximity effect, when the two d -wave order parameters mixed near the boundary are spatially rotated by a nontrivial angle $\delta\chi$ and have a nontrivial phase shift $\pm\phi_0 \neq 0, \pi$. Although the argument given here is based on having a mixed order parameter near the boundary region, in fact the presence of the second order parameter is not necessary. The reason is that the subdominant symmetry already exists in the Green’s functions g_ω and f_ω ,

even if the interaction potential does not support pairing in that channel. Since the current density is related to these functions rather than to the pairing potential [cf. Eq. (A5)], the molecular current is basically formed by inherently mixed symmetries of these functions.

The above arguments are certainly not true when the order parameter symmetry is $d + is$, as in SD junctions (Fig. 7a). In this case the molecular current is identically zero and as a result no countercurrent exists. (Of course, since the Meissner currents must be taken into account in this case, the results are valid only if the system size is much less than the London penetration depth.)

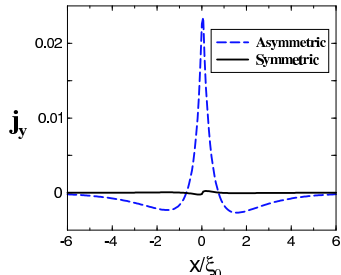


FIG. 9. Comparison between the size of the spontaneous current in asymmetric and symmetric $\delta\chi = 45^\circ$ DD junctions. Both calculations are done at $t = 0.5$.

An interesting case is presented by a symmetric 45° -junction ($\chi_l = -22.5^\circ$ and $\chi_r = 22.5^\circ$). Although the ground state is degenerate in this case [23], the spontaneous current is practically absent (Fig. 9). This is easy to see from geometric considerations (Fig. 1c). Consider the total supercurrent across the boundary as a sum of contributions from quasiclassical trajectories. There are two groups, analogous to Andreev regular and π -levels discussed in the introduction; the corresponding directions are within the shaded and white sectors in Fig. 1c respectively. In equilibrium, their contributions to the current normal to the boundary must cancel each other. What happens to the tangential component of the equilibrium (spontaneous) current, depends on the orientations of the order parameters with respect to the boundary and each other, and the equilibrium phase difference (also a function of temperature). It is obvious from the picture that for any given mismatch angle $\delta\chi$, in a *symmetric* junction, the tangential components of the current cancel for regular and π -directions *separately*. This is why symmetric junctions are very “quiet” (using the term of [39]): they can violate \mathcal{T} -symmetry without producing local magnetic fields, which could couple to some external degrees of freedom [40]. This can be both an advantage and a disadvantage from the point of view of using such a system as a solid-state qubit [39,30].

B. Reflective junctions

We also study the properties of the spontaneous current in the presence of a non-ideal boundary, i.e., with nonunity transparency and/or surface roughness. The details of our method of numerical calculation are given in appendix C. The transparency and roughness of the boundary are parameterized by $0 \leq D_0 \leq 1$ and $0 \leq \rho < \infty$ respectively (see appendix C for definitions). In particular, in the case of a clean ideal junction, $D_0 = 1$ and $\rho = 0$.

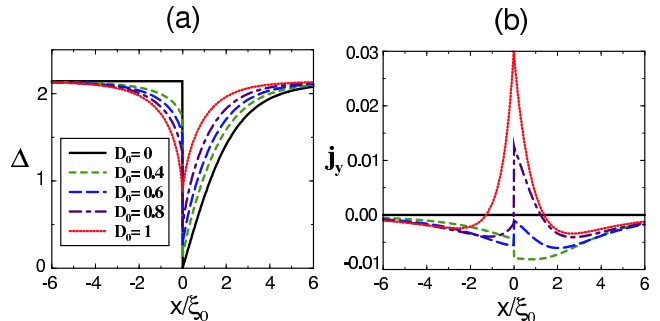


FIG. 10. Order parameter (a) and spontaneous current distribution (b) in $(0^\circ - 45^\circ)$ asymmetric grain boundary junctions with different transparencies D_0 at $t = 0.1$.

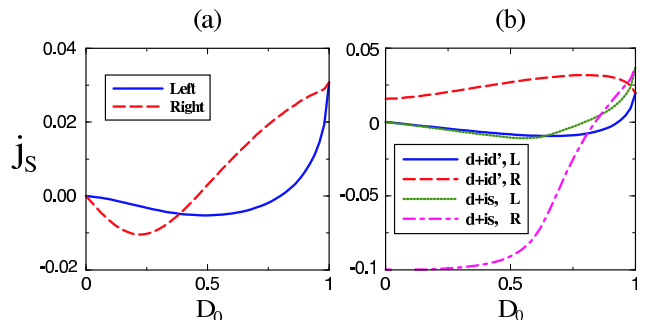


FIG. 11. Influence of finite barrier transparency on spontaneous current amplitude in an asymmetric $(0^\circ - 45^\circ)$ DD junction without (a) and with (b) subdominant order parameter. Here “L” = *left* and “R” = *right* of the boundary and the calculations are done at $t = 0.05$ and $t_{c2} = 0.1$ (for (b)). In the case of (b), one can see that as $D_0 \rightarrow 0$, the spontaneous currents on the right hand side of the boundary survive.

In Fig. 10a we see the self-consistent pairing potential near the interface for several values of D_0 . Notice that for the case of $D_0 = 0$ (i.e., totally reflecting surface), the order parameter is constant on the left while it vanishes at the junction on the right side of the boundary. The latter is because the quasiparticles on the right see opposite sign of the order parameter after reflection from the boundary [35]. As $D_0 \rightarrow 1$, the order parameter becomes continuous at the boundary. The spontaneous

current (Fig. 10b) also evolves from zero to its maximum value as D_0 changes from 0 to 1. Notice that at all values of D_0 except for 0 and 1, the magnitudes of the spontaneous current on the left and right hand sides of the boundary are different and exact superscreening happens only in the ideal boundary case ($D_0 = 1$). Fig. 11a demonstrates the continuous evolution of the spontaneous current from zero to its maximum as a function of D_0 . This picture is influenced by the presence of a subdominant interaction in Fig. 11b. Especially, on the right hand side of the junction (with $\chi_r = 45^\circ$ orientation), the spontaneous current does not vanish even at $D_0 = 0$. We will come back to this point in the next section.

C. Rough junctions

The effect of surface roughness is very different from that of finite transparency. First notice from Fig. 12 that surface roughness has little effect on the order parameter distribution (Fig. 12a), while it significantly changes the spontaneous current (Fig. 12b). This may seem strange, until we recall that supercurrents (including spontaneous currents) are generated not by the order parameter Δ , but by the Green's functions, f_ω and g_ω [related by the normalization condition (A3)]. The latter *is* directly affected by the boundary roughness, while the former isn't. Again, we notice that exact superscreening is absent at finite roughness.

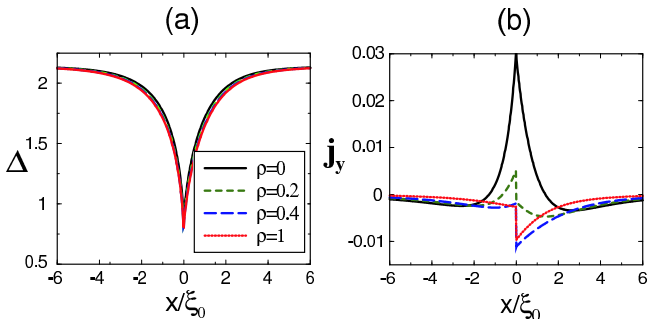


FIG. 12. Order parameter (a) and spontaneous current distribution (b) in $(0^\circ\text{-}45^\circ)$ asymmetric grain boundary junction with different values of the surface roughness ρ at $t = 0.1$.

Another interesting effect is presented in Fig. 13a: as the surface becomes rougher and rougher ($\rho \rightarrow \infty$), the spontaneous current on the left side (with $\chi_l = 0$) vanishes while on the right side ($\chi_r = 45^\circ$) it saturates to a finite value. This non-trivial behavior is directly related to the anomalous proximity effect between a d -wave superconductor and a disordered region studied by Golubov and Kupriyanov [36]. When ρ is large, the contributions from different quasiclassical trajectories are mixed. Therefore the angle-dependent components of f , which “leak” through the boundary to the other side, are suppressed, but in the limit of infinite roughness the s -wave

contribution still survives. The latter is generated by scattering from the rough boundary even in case of only dominant d -wave pairing on either side, and can be estimated as $f_{s,\text{eff}} = \int_{-\pi/2}^{\pi/2} (d\theta/\pi) \cos \theta f(\theta, 0^\pm)$ [the upper (lower) sign corresponds to leakage from the right (left) to the left (right) side of the junction]. In an asymmetric $(0^\circ\text{-}45^\circ)$ DD junction we thus expect exactly zero induced f on the left due to symmetry, while on the right a finite s -wave component should appear with amplitude $2/(3\pi) \approx 0.2$ relative to the d -wave anomalous Green's function across the boundary. The spontaneous currents in this case can flow only on the right of the boundary, where the chiral combination $d \pm is$ is thus formed, in agreement with our numerical results. This might also explain why superscreening is absent in case of rough surfaces: $d + is$ symmetry does not support molecular moments. Non-ideal asymmetric grain boundaries between d -wave superconductors can thus be better candidates for the search of spontaneous currents, since the superscreening is suppressed, while the supercurrent amplitudes are still detectable.

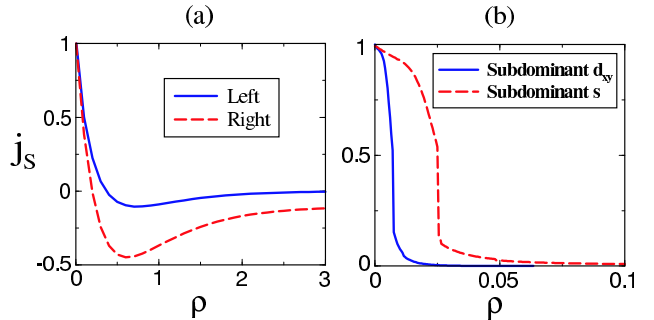


FIG. 13. Influence of surface/interface roughness on the magnitude of spontaneous current in a junction (a) and near a surface (b). Note that in the latter case spontaneous currents are suppressed at much smaller values of ρ . All calculations are done at $t = 0.1$

III. SPONTANEOUS CURRENT GENERATED BY SUBDOMINANT ORDER PARAMETER

We already saw the effect of the presence of a subdominant order parameter on the spontaneous current in DD grain boundary junctions (Fig. 6). In particular in Fig. 6b we notice that the subdominant component exists even at temperatures above the subdominant critical temperature, T_{c2} . The subdominant order parameter in Fig. 6b is therefore completely induced by the proximity to a differently oriented superconductor on the other side of the junction. On the other hand, in Fig. 11b we realized that the spontaneous current exists even when $D_0 \rightarrow 0$, i.e., when the proximity effect is completely absent. This happens only when $T < T_{c2}$ and therefore the mechanism is completely different from the one described above.

In general, the bulk of a superconductor can support only one symmetry of the order parameter even if the interaction potential contains finite interaction in several different channels (unless the coupling constants of the channels are very close to each other [37]). This is because the dominant order parameter introduces a cutoff, in the BCS gap equation, that removes the logarithmic divergence (at small ω), responsible for the exponential dependence of the gap on the interaction potential (see appendix D). As we saw in Fig. 10a, at a reflective surface of a 45° oriented d -wave superconductor, the dominant order parameter vanishes. Suppression of the dominant order parameter gives the chance to the next subdominant one to appear if the temperature is below its corresponding critical temperature. Thus, the appearance of subdominant order involves a spontaneous symmetry breaking and therefore a second order phase transition. This is demonstrated in Fig. 14b (we increase T_{c2} instead of T in that figure, but the behavior is the same). The subdominant order parameter always appears with a phase $\pi/2$ with respect to the main one. With this phase difference, the mixed order parameter ($d_{x^2-y^2} \pm id_{xy}$ or $d_{x^2-y^2} \pm is$) is fully gapped (with no nodes), which is energetically favorable because of the extra condensation energy gained.

It is important to notice that the above phenomenon is not likely to happen at the interface between superconductors because the dominant order parameter is never completely suppressed (except when $D = 0$, cf. Fig. 10a). Even at rough interfaces, the dominant order parameter at the boundary is only slightly less than half of its bulk value (Fig. 12a). The subdominant order parameter in this case is predominantly induced by the proximity effect and therefore follows the symmetry of the neighboring superconductor. This may explain why the mixed symmetry state was not observed in a recent experiment [38].

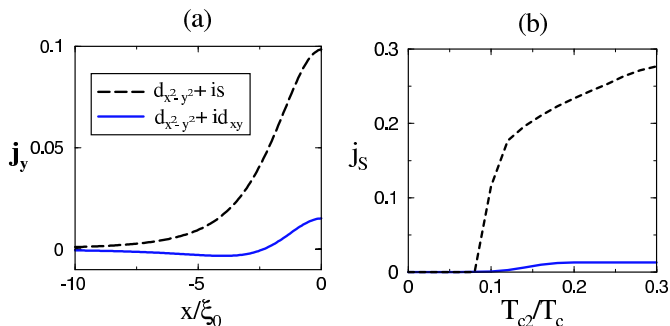


FIG. 14. (a) Spontaneous current profile near the (110)-surface of a d -wave superconductor with d_{xy} - and s -wave subdominant order parameter. Here $t = 0.05$ and $t_{c2} = 0.1$ for both the s and d_{xy} subdominant gaps. (b) Spontaneous current at the surface as a function of the subdominant transition temperature at $t = 0.1$.

Spontaneous currents at a surface of a d -wave super-

conductor are presented in Fig. 14a. Qualitatively, they are the same as at a DD or DS boundary, with the same superscreening behavior in the case of $d + id'$ order parameter symmetry. Despite the similarities in the current distribution, there are fundamental differences between the two cases. First of all, unlike at the interface, the appearance of spontaneous current near the surface is a very fragile phenomenon. A small deviation from the 45° angle will suppress the effect significantly. It is also very sensitive to surface roughness as compared to the interface current; a small ρ is enough to remove the spontaneous current (Fig. 13b). Moreover, unless the effects of the magnetic field generated by spontaneous currents itself are taken into account, the presence of a subdominant gap is necessary for the surface spontaneous current, but not for the interface one. (The spontaneous symmetry breaking due to Doppler shifts of midgap states [41] occurs at temperatures below $1/6\Delta(\xi_0/\lambda_L)$ [42–44], that is approximately 1K for high- T_c compounds.)

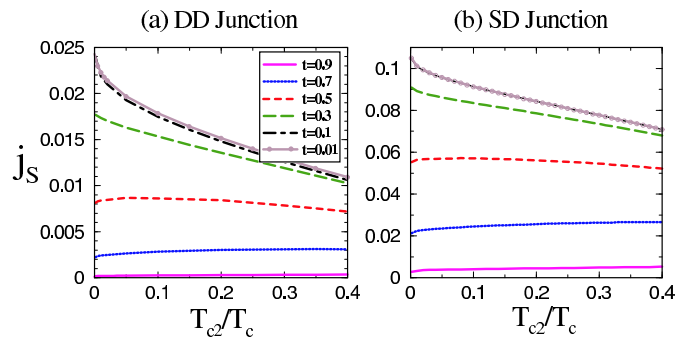


FIG. 15. Suppression of spontaneous currents in the presence of subdominant order parameter as a function of subdominant transition temperature. In both cases we have taken the same T_c on both side of the junction.

It is interesting to note that the presence of interaction in a subdominant channel actually works *against* the appearance of spontaneous current at an interface [24]. This behavior is displayed for both DD and SD junctions in Fig. 15. The reason becomes clear from considering the Andreev levels in the junction (which can be modeled on this occasion by a DND junction, Fig. 16). The induced subdominant order parameter will be aligned with the dominant one across the boundary. Therefore in addition to the “dominant-dominant” set of Andreev levels there will appear a “subdominant-subdominant” set, which obviously carries supercurrents in the *opposite* direction. Of course, a subdominant pairing potential should also suppress the Josephson current, which was indeed noted in [45].

As we have mentioned above, the subdominant order parameter near interfaces is induced across the boundary from the other side, where it is dominant, and can be suppressed only simultaneously with the latter. Therefore, it seems impossible to directly observe the influence of the subdominant order on the spontaneous currents by e.g.

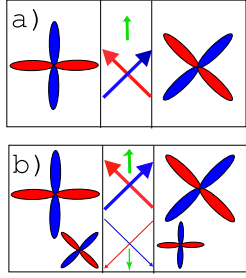


FIG. 16. The physical mechanism of spontaneous current suppression by subdominant order parameter in DND model (see text).

raising the temperature above T_{c2} to suppress it. The same, of course, holds true for suppression by magnetic field.

IV. CONCLUSIONS

We have investigated the occurrence of spontaneous currents at surfaces and interfaces of d -wave superconductors, using the self-consistent quasiclassical Eilenberger equations. A \mathcal{T} -breaking ground state is the only necessary condition for their appearance, with no quantization condition for the generated magnetic fluxes. Therefore, the effect is sensitive to the properties of the system and allows the existence of “quiet” \mathcal{T} -breaking states, i.e., states with fluxes much smaller than the flux quantum.

We have shown that the spontaneous current at the (110)-surface of a d -wave superconductor is formed through a second order phase transition to a mixed symmetry state ($d + id'$ or $d + is$), and is very sensitive to the interaction in the subdominant channel, temperature, and surface roughness and reflectivity. On the other hand, at an interface between two differently oriented d -wave superconductors, or between a d -wave and an s -wave superconductor, the spontaneous current is generated as a result of the proximity effect. It is generally robust, with less sensitivity to the above effects. In particular, at very rough surfaces, the spontaneous current survives on one side of the junction, in agreement with the recently proposed anomalous proximity effect at rough d -wave surfaces. We also show that interaction in any subdominant channel suppresses the spontaneous current at the interface, while its existence is necessary for the \mathcal{T} -breaking at the surfaces.

The contribution to the spontaneous current from the local orbital moment of the condensate leads to characteristic “superscreening” of the equilibrium current in DD junctions and at surfaces with d_{xy} subdominant order. Exact superscreening is sensitive to boundary imperfections and disappears at finite roughness and/or nonunity transparency of the junction.

ACKNOWLEDGMENT

We are grateful to I. Affleck, Ya. Fominov, A. Golubov, Yu. Gusev, W. Hardy, E. Il'ichev, G. Rose, and A. Smirnov for enlightening discussions, and A. Maassen van den Brink for carefully reading this manuscript and many helpful remarks. M.A. would also like to thank I. Herbut for stimulating conversations. A.Z. gratefully appreciates valuable comments by T. Löfwander and J. Hogan-O'Neill.

APPENDIX A: QUASICLASSICAL EILENBERGER EQUATIONS

To describe the coherent current states in a superconducting ballistic microstructure we use the Eilenberger equations for the ξ -integrated Green's functions [31]:

$$\mathbf{v}_F \cdot \frac{\partial}{\partial \mathbf{r}} \hat{G}_\omega(\mathbf{v}_F, \mathbf{r}) + [\omega \hat{\tau}_3 + \hat{\Delta}(\mathbf{v}_F, \mathbf{r}), \hat{G}_\omega(\mathbf{v}_F, \mathbf{r})] = 0, \quad (\text{A1})$$

where

$$\hat{\Delta} = \begin{pmatrix} 0 & \Delta \\ \Delta^\dagger & 0 \end{pmatrix}, \quad \hat{G}_\omega(\mathbf{v}_F, \mathbf{r}) = \begin{pmatrix} g_\omega & f_\omega \\ f_\omega^\dagger & -g_\omega \end{pmatrix}. \quad (\text{A2})$$

Δ is the superconducting order parameter and $\hat{G}_\omega(\mathbf{v}_F, \mathbf{r})$ is the matrix Green's function, which depends on the electron velocity on the Fermi surface \mathbf{v}_F , the coordinate \mathbf{r} and the Matsubara frequency $\omega = (2n + 1)\pi T$, with n being an integer number and T the temperature. We also need to satisfy the normalization condition

$$g_\omega = \sqrt{1 - f_\omega f_\omega^\dagger}. \quad (\text{A3})$$

In general, Δ depends on the direction of \mathbf{v}_F and is determined by the self-consistency equation

$$\Delta(\mathbf{v}_F, \mathbf{r}) = 2\pi N(0)T \sum_{\omega > 0} \langle V(\mathbf{v}_F, \mathbf{v}'_F) f_\omega(\mathbf{v}'_F, \mathbf{r}) \rangle_{\mathbf{v}'_F} \quad (\text{A4})$$

where $V(\mathbf{v}_F, \mathbf{v}'_F)$ is the interaction potential. Solution of matrix equation (A1) together with (A4) determines the current density $\mathbf{j}(\mathbf{r})$ in the system

$$\mathbf{j}(\mathbf{r}) = -4\pi i e N(0)T \sum_{\omega > 0} \langle \mathbf{v}_F g_\omega(\mathbf{v}_F, \mathbf{r}) \rangle_{\mathbf{v}_F}. \quad (\text{A5})$$

In two dimensions, $N(0) = m/2\pi$ is the 2D density of states and $\langle \dots \rangle = \int_0^{2\pi} (d\theta/2\pi) \dots$ is the averaging over directions of 2D vector \mathbf{v}_F . Throughout this article we write current densities in units of

$$j_c \equiv 4\pi |e| v_F N(0) T_c \quad (\text{A6})$$

which is of the order of the bulk critical current density.

Supposing $\Delta(-\mathbf{v}_F) = \Delta(\mathbf{v}_F)$, which is always the case for superconductors with singlet pairing, from the equation of motion (A1) and Eq. (A3) we have the following symmetry relations:

$$\begin{aligned} f^*(-\omega) &= f^\dagger(\omega), \\ g^*(-\omega) &= -g(\omega), \\ f^*(\omega, -\mathbf{v}_F) &= f^\dagger(\omega, \mathbf{v}_F), \\ g^*(\omega, -\mathbf{v}_F) &= g(\omega, \mathbf{v}_F), \\ f(-\omega, -\mathbf{v}_F) &= f(\omega, \mathbf{v}_F), \\ g(-\omega, -\mathbf{v}_F) &= -g(\omega, \mathbf{v}_F), \\ \Delta^\dagger &= \Delta^*. \end{aligned}$$

APPENDIX B: NON-SELF-CONSISTENT ANALYTICAL SOLUTION

We assume a boundary, at $x = 0$, between two superconductors. To find an analytical solution we neglect the self-consistency equation (A4), and write

$$\Delta(\mathbf{v}_F, x) = \begin{cases} \Delta_l(\mathbf{v}_F) \exp(i\phi/2), & x < 0 \\ \Delta_r(\mathbf{v}_F) \exp(-i\phi/2), & x > 0 \end{cases}, \quad (\text{B1})$$

where l (r) stands for left (right) of the boundary. $\Delta_{l,r}$ can in general have d -wave, s -wave, or any other symmetries. The Eilenberger equations for the Green's function \hat{G}_ω are linear and therefore can be easily solved separately for positive and negative x to satisfy

$$\lim_{x \rightarrow \mp\infty} f_\omega = \frac{\Delta_{l,r}}{\Omega_{l,r}}, \quad \lim_{x \rightarrow \mp\infty} g_\omega = \frac{\omega}{\Omega_{l,r}}, \quad (\text{B2})$$

where $\Omega_{l,r} = \sqrt{\omega^2 + |\Delta_{l,r}|^2}$. This yields the following solutions. For $x \leq 0$

$$\begin{aligned} f(x, \theta) &= \frac{\Delta_l e^{i\phi/2}}{\Omega_l} + \frac{e^{i\phi/2}}{\Delta_l} (\eta\Omega_l - \omega) e^{2x\Omega_l/|v_x|} C_1 \\ f^\dagger(x, \theta) &= \frac{\Delta_l e^{-i\phi/2}}{\Omega_l} + \frac{e^{-i\phi/2}}{\Delta_l} (-\eta\Omega_l - \omega) e^{2x\Omega_l/|v_x|} C_1 \\ g(x, \theta) &= \frac{\omega}{\Omega_l} + e^{2x\Omega_l/|v_x|} C_1, \end{aligned} \quad (\text{B3})$$

for $x \geq 0$

$$\begin{aligned} f(x, \theta) &= \frac{\Delta_r e^{-i\phi/2}}{\Omega_r} + \frac{e^{-i\phi/2}}{\Delta_r} (-\eta\Omega_r - \omega) e^{-2x\Omega_r/|v_x|} C_2 \\ f^\dagger(x, \theta) &= \frac{\Delta_r e^{i\phi/2}}{\Omega_r} + \frac{e^{i\phi/2}}{\Delta_r} (\eta\Omega_r - \omega) e^{-2x\Omega_r/|v_x|} C_2 \\ g(x, \theta) &= \frac{\omega}{\Omega_r} + e^{-2x\Omega_r/|v_x|} C_2. \end{aligned} \quad (\text{B4})$$

Here $\eta \equiv \text{sign}(v_x)$. Imposing the continuity condition for \hat{G}_ω at the boundary we find

$$\begin{aligned} C_1 &= \frac{\Delta_l \omega (\Delta_l - \Delta_r \cos \phi) - i\eta \Delta_r \Omega_l \sin \phi}{\Omega_l (\Omega_l \Omega_r + \omega^2 + \Delta_l \Delta_r \cos \phi)} \\ C_2 &= \frac{\Delta_r \omega (\Delta_r - \Delta_l \cos \phi) - i\eta \Delta_l \Omega_r \sin \phi}{\Omega_r (\Omega_l \Omega_r + \omega^2 + \Delta_l \Delta_r \cos \phi)}. \end{aligned} \quad (\text{B5})$$

Substituting into (B3) or (B4) at $x = 0$ we find the Green's functions f and g to be

$$f(0) = \frac{\Delta_l (\Omega_r + \eta\omega) e^{i\phi/2} + \Delta_r (\Omega_l + \eta\omega) e^{-i\phi/2}}{\Omega_l \Omega_r + \omega^2 + \Delta_l \Delta_r \cos \phi}, \quad (\text{B6})$$

$$g(0) = \frac{\omega (\Omega_l + \Omega_r) - i\eta \Delta_l \Delta_r \sin \phi}{\Omega_l \Omega_r + \omega^2 + \Delta_l \Delta_r \cos \phi}. \quad (\text{B7})$$

Using the expressions (A4) and (B7), we obtain the current densities $j_x(0) \equiv j_J$ and $j_y(0) \equiv j_S$

$$j_J = t \sum_{\omega > 0} \left\langle \frac{\Delta_l \Delta_r |\cos \theta|}{\Omega_l \Omega_r + \omega^2 + \Delta_l \Delta_r \cos \phi} \right\rangle_\theta \sin \phi, \quad (\text{B8})$$

$$j_S = t \sum_{\omega > 0} \left\langle \frac{\Delta_l \Delta_r \sin \theta \text{sign}(\cos \theta)}{\Omega_l \Omega_r + \omega^2 + \Delta_l \Delta_r \cos \phi} \right\rangle_\theta \sin \phi, \quad (\text{B9})$$

where the current densities are in units of j_c [defined in (A6)] and $t \equiv T/T_c$. At all other points we can find \mathbf{j} from

$$\mathbf{j}(x) = t \sum_{\omega > 0} \left\langle \frac{\hat{v}_F \eta \Delta_l \Delta_r \sin \phi e^{-2|x|\Omega_r/|v_F \cos \theta|}}{\Omega_l \Omega_r + \omega^2 + \Delta_l \Delta_r \cos \phi} \right\rangle_\theta \quad (\text{B10})$$

where \hat{v}_F is a unit vector in the direction of \mathbf{v}_F .

APPENDIX C: SELF-CONSISTENT NUMERICAL SOLUTION

The general approach we use is based on transformation of the set of coupled (formally) linear Eilenberger equations (A1) for the functions f, f^\dagger, g to two nonlinear, but separate, equations which are numerically stable (Schopohl-Maki transformation [46]). To this end we express the components of \hat{G}_ω matrix as

$$g = \frac{1-ab}{1+ab}, \quad f = \frac{2a}{1+ab}, \quad f^\dagger = \frac{2b}{1+ab}. \quad (\text{C1})$$

Now a and b satisfy two independent nonlinear equations

$$\begin{aligned} \mathbf{v}_F \cdot \nabla a &= \Delta - \Delta^* a^2 - 2\omega a \\ -\mathbf{v}_F \cdot \nabla b &= \Delta^* - \Delta b^2 - 2\omega b. \end{aligned} \quad (\text{C2})$$

Notice from these equations that $a(-\mathbf{v}_F) = b^*(\mathbf{v}_F)$ and $b(-\mathbf{v}_F) = a^*(\mathbf{v}_F)$. We use the solutions for a homogeneous system,

$$a = \frac{\Delta}{\omega + \Omega}, \quad b = \frac{\Delta^*}{\omega + \Omega} \quad (\text{C3})$$

where $\Omega = \sqrt{\omega^2 + |\Delta|^2}$, as asymptotic conditions at $x \rightarrow \pm\infty$. For positive v_x , the first (second) of Eqs.

(C2) is stable if we choose the boundary condition at $-\infty$ ($+\infty$). Using the appropriate asymptotic condition one can find a (b) at all other points on the quasiclassical trajectory along the vector \mathbf{v}_F , integrating along the trajectory. Self-consistency is achieved iteratively. The step-like approximation (B1) is used to find a, b in the first approximation, which are in turn substituted in Eq. (A4) to find the next iteration for Δ . These steps are repeated until Δ does not change within numerical accuracy.

It is convenient to take the order parameter constant between discrete points on the trajectory (the angle θ gives the direction of \mathbf{v}_F as usual), separated by a distance h . Then we find

$$\begin{aligned} a_{i+1} &= a_i + \frac{\Delta_i - a_i^2 \Delta_i^* - 2a_i \omega}{a_i \Delta_i^* + \omega + \Omega_i \coth(\Omega_i h / \cos \theta)}, \\ b_{i-1} &= b_i + \frac{\Delta_i^* - b_i^2 \Delta_i - 2b_i \omega}{b_i \Delta_i + \omega + \Omega_i \coth(\Omega_i h / \cos \theta)}. \end{aligned} \quad (\text{C4})$$

(We have explicitly taken into account that this procedure is stable in opposite directions for a, b). Having obtained a and b , we can find f and g and therefore the order parameter Δ and current density \mathbf{j} using (A4) and (A5).

1. Effect of surface reflectivity

Our numerical method can also be applied when the transparency of the junction is arbitrary, $0 \leq D \leq 1$. Since part of the quasiparticles get reflected from the boundary, the quasiparticle trajectories of the reflected quasiparticles and the transmitted ones from the other side will mix. Then even in the non-self-consistent approximation for the order parameter (B1) we cannot simply impose continuity of the Green's functions along a trajectory as we did before for the ideal transparency case. Instead, one should use Zaitsev's boundary conditions [47] which for $v_x > 0$ is given by [48]

$$\hat{d}^l = \hat{d}^r \equiv \hat{d} \quad (\text{C5})$$

$$\frac{D}{2-D} \left[\left(1 + \frac{\hat{d}}{2} \right) \hat{s}^r, \hat{s}^l \right] = \hat{d} \hat{s}^l \quad (\text{C6})$$

where

$$\begin{aligned} \hat{s}^r &= \hat{G}_\omega^r(\mathbf{v}_F, x=0) + \hat{G}_\omega^r(\mathbf{v}'_F, x=0) \\ \hat{d}^r &= \hat{G}_\omega^r(\mathbf{v}_F, x=0) - \hat{G}_\omega^r(\mathbf{v}'_F, x=0) \end{aligned} \quad (\text{C7})$$

with \mathbf{v}'_F being the reflection of \mathbf{v}_F with respect to the boundary. Similar relations also hold for \hat{s}^l and \hat{d}^l . For $v_x < 0$ one has to replace $r \leftrightarrow l$ in (C6). In general, D can be momentum dependent. In our calculations we consider [19]

$$D(\theta) = \frac{D_0 \cos^2 \theta}{1 - D_0 \sin^2 \theta}. \quad (\text{C8})$$

Let us introduce four Green's functions

$$\begin{aligned} \hat{G}_1 &= \hat{G}_\omega(0_-, \theta), & \hat{G}_3 &= \hat{G}_\omega(0_-, \pi - \theta) \\ \hat{G}_2 &= \hat{G}_\omega(0_+, \theta), & \hat{G}_4 &= \hat{G}_\omega(0_+, \pi - \theta) \end{aligned} \quad (\text{C9})$$

We can now write

$$\begin{aligned} \hat{s}^l &= \hat{G}_1 + \hat{G}_3, & \hat{d}^l &= \hat{G}_1 - \hat{G}_3 \\ \hat{s}^r &= \hat{G}_2 + \hat{G}_4, & \hat{d}^r &= \hat{G}_2 - \hat{G}_4 \end{aligned} \quad (\text{C10})$$

Rewriting these Green's functions in terms of a_ν, b_ν ($\nu = 1, \dots, 4$), we can calculate a_1, b_2, b_3 , and a_4 by integrating from the corresponding infinity in the direction of convergence [e.g. using Eq. (C4)]. At the boundary, the remaining functions b_1, a_2, a_3 , and b_4 are obtained from Zaitsev's boundary conditions; the remarkable results obtained by Eschrig [49] are

$$\begin{aligned} b_1 &= \frac{Db_2 + Rb_3 + a_4 b_2 b_3}{1 + a_4 (Db_3 + Rb_2)}, & a_2 &= \frac{Da_1 + Ra_4 + a_1 a_4 b_3}{1 + b_3 (Da_4 + Ra_1)}, \\ a_3 &= \frac{Da_4 + Ra_1 + a_1 a_4 b_2}{1 + b_2 (Da_1 + Ra_4)}, & b_4 &= \frac{Db_3 + Rb_2 + a_1 b_2 b_3}{1 + a_1 (Db_2 + Rb_3)}. \end{aligned}$$

Notice that $D = 1$ gives: $a_1 = a_2$, $a_3 = a_4$, and $D = 0$ gives: $a_1 = a_3$, $a_2 = a_4$, which correspond to the completely transparent and completely reflective cases respectively (the same argument also holds for the b 's). The values of the a 's and b 's at other points are calculated using Eq. (C4).

2. Effect of surface roughness

The effects of surface roughness are accounted for by introducing a thin layer of impurities (elastic scatterers) of width d [50–52]. In the Born approximation, the Eilenberger equations in the layer are written as

$$\begin{aligned} \mathbf{v}_F \cdot \frac{\partial}{\partial \mathbf{r}} \hat{G}_\omega(\mathbf{v}_F, \mathbf{r}) + \left[\omega_R \hat{\tau}_3 + \hat{\Delta}_R(\mathbf{v}_F, \mathbf{r}), \hat{G}_\omega(\mathbf{v}_F, \mathbf{r}) \right] &= 0; \\ \hat{\Delta}_R &= \begin{pmatrix} 0 & \Delta_R \\ \Delta_R^* & 0 \end{pmatrix}, \end{aligned} \quad (\text{C11})$$

where

$$\omega_R(x) = \omega + \frac{\langle g_\omega(\mathbf{v}_F, x) \rangle_{\mathbf{v}_F}}{2\tau}, \quad \Delta_R(x) = \Delta + \frac{\langle f_\omega(\mathbf{v}_F, x) \rangle_{\mathbf{v}_F}}{2\tau},$$

$\tau = v_F l$, and l is the mean free path inside the layer. The degree of roughness is given by the ratio $\rho = d/l$ in the limit when $d \rightarrow 0, l \rightarrow 0$ simultaneously. For strong scattering, the x -independent terms in the above expressions can be dropped to obtain the Schopohl-Maki transformed equations in the form

$$\begin{aligned} -\cos \theta \frac{\partial a}{\partial x} &= 2\tilde{\omega} a - \tilde{\Delta} + \tilde{\Delta}^* a^2; \\ \cos \theta \frac{\partial b}{\partial x} &= 2\tilde{\omega} b - \tilde{\Delta}^* + \tilde{\Delta} b^2, \end{aligned} \quad (\text{C12})$$

where $\tilde{x} = x/d$ and

$$\tilde{\omega}(\tilde{x}) = \frac{1}{2}\rho \langle g_\omega(\mathbf{v}_F, \tilde{x}d) \rangle_{\mathbf{v}_F}, \quad \tilde{\Delta}(\tilde{x}) = \frac{1}{2}\rho \langle f_\omega(\mathbf{v}_F, \tilde{x}d) \rangle_{\mathbf{v}_F}.$$

In the above mentioned limit, integrating the equations over \tilde{x} from 0 to 1, and assuming that f_ω, g_ω are slow functions of x , we can use Eq. (C4) with $h = 1$ to calculate the jump of a_ν, b_ν across the boundary. This approach also works for a rough surface (we put formally $D = 0$).

APPENDIX D: ORDER PARAMETERS IN A D -WAVE SUPERCONDUCTOR

As mentioned in appendix A, the order parameter in a superconductor is related to the anomalous Green's function via the self-consistency equation (A4). In general the interaction potential $V(\mathbf{v}_F, \mathbf{v}'_F)$ in (A4) can have components in different channels. Keeping only the important terms, we can write

$$V(\mathbf{v}_F, \mathbf{v}'_F) = V_d \cos 2\theta \cos 2\theta' + V_{d'} \sin 2\theta \sin 2\theta' + V_s \quad (D1)$$

where $V_d, V_{d'}$, and V_s are the components of the interaction potential in the $d_{x^2-y^2}, d_{xy}$, and s channels respectively. (In these expressions we assume $x \parallel \mathbf{a}$ and $y \parallel \mathbf{b}$, since the orientation of the order parameter is linked to the local crystal axes of the system \mathbf{a}, \mathbf{b} .) The order parameter in this case can also have mixed symmetry

$$\Delta(\mathbf{v}_F, \mathbf{r}) = \Delta_d(\mathbf{r}) \cos 2\theta + \Delta_{d'}(\mathbf{r}) \sin 2\theta + \Delta_s(\mathbf{r}) \quad (D2)$$

Substituting into (A4) we find

$$\Delta_d(\mathbf{r}) = 4\pi\lambda_d T \sum_{\omega>0} \int \frac{d\theta}{2\pi} f_\omega(\theta, \mathbf{r}) \cos 2\theta \quad (D3)$$

$$\Delta_{d'}(\mathbf{r}) = 4\pi\lambda_{d'} T \sum_{\omega>0} \int \frac{d\theta}{2\pi} f_\omega(\theta, \mathbf{r}) \sin 2\theta \quad (D4)$$

$$\Delta_s(\mathbf{r}) = 2\pi\lambda_s T \sum_{\omega>0} \int \frac{d\theta}{2\pi} f_\omega(\theta, \mathbf{r}) \quad (D5)$$

where $\lambda_{d,d'} = N(0)V_{d,d'}/2$ and $\lambda_s = N(0)V_s$ are dimensionless interaction constants. These equations are used in the self-consistent calculation of the components of the order parameter.

In a homogeneous superconductor, the anomalous Green's function f_ω takes the simple form

$$f_\omega(\theta) = \frac{\Delta(\theta)}{\sqrt{\omega^2 + |\Delta(\theta)|^2}} \quad (D6)$$

Keeping only the $d_{x^2-y^2}$ component of the order parameter we find

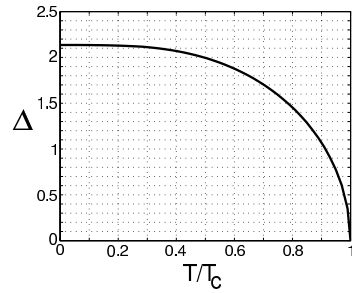


FIG. 17. Superconducting gap as a function of temperature.

$$\Delta_d(T) = \lambda_d 4\pi T \sum_{\omega>0}^{\omega_c} \int_0^{2\pi} \frac{d\theta}{2\pi} \frac{\Delta_d(T) \cos^2 2\theta}{\sqrt{\omega^2 + \Delta_d(T)^2 \cos^2 2\theta}} \quad (D7)$$

where ω_c is the cutoff frequency. In our numerical calculations we take $\omega_c = 10\pi$. At $T = 0$, the right hand side of Eq. (D7) diverges as $\Delta_d \rightarrow 0$. Thus, no matter how small λ_d is, there exists a finite value for Δ_d that satisfies Eq. (D7). There also exists a finite temperature T_c , below which Δ_d is nonzero. This is not true for the subdominant order parameters, because the presence of the dominant order parameter, at $T < T_c$, introduces a cutoff which removes the divergence. As a result, even below T_{c2} , the bulk of the superconductor contains only one symmetry of the order parameter (the dominant one) even if the interaction potential supports other symmetries as well [26]. Near a (110)-surface of a d -wave superconductor on the other hand, the dominant order parameter is suppressed and subdominant gaps may appear. The resulting mixed order parameter (e.g. $d + id'$ or $d + is$) breaks time reversal symmetry and results in spontaneous currents near the surface. This behavior is clearly demonstrated in Fig. 14a.

One can show that λ_d is related to T_c by

$$\lambda_d^{-1} = \ln \frac{T}{T_c} + 2\pi T \sum_{\omega>0}^{\omega_c} \frac{1}{\omega} \quad (D8)$$

The same equation holds for other symmetries of the order parameter. In our numerical calculations we use (D8) to find $\lambda_{d'}$ and λ_s from T_{c2} and T_{cs} respectively.

At $T = 0$, and in the weak coupling limit $\lambda_d \ll 1$, it follows from (D7) that

$$\Delta_d(0) = 2\omega_c \beta e^{-1/\lambda_d}, \quad \ln \beta = \ln 2 - 1/2 \approx 1.21. \quad (D9)$$

The critical temperature T_c on the other hand is

$$T_c = \frac{2}{\pi} \omega_c \gamma e^{-1/\lambda_d}, \quad \ln \gamma = 0.577, \quad \gamma \approx 1.78. \quad (D10)$$

Thus, $\Delta_d(0)/T_c = \pi\beta/\gamma \approx 2.14$. In terms of T_c , Eq. (D7) can be presented in the form :

$$\ln \frac{T}{T_c} = 2\pi T \sum_{\omega>0}^{\infty} \left(2 \int_0^{2\pi} \frac{d\theta}{2\pi} \frac{\cos^2 2\theta}{\sqrt{\omega^2 + \Delta_d(T)^2 \cos^2 2\theta}} - \frac{1}{\omega} \right)$$

In the limiting cases, the solution of this equation reads

$$\Delta_d(T) = \begin{cases} \Delta_d(0) [1 - 3\zeta(3)] \left(\frac{T}{\Delta_d(0)}\right)^3, & T \ll T_c \\ \left(\frac{32\pi^2}{21\zeta(3)}\right)^{1/2} T_c (1 - \frac{T}{T_c})^{1/2}, & T \lesssim T_c \end{cases}$$

For arbitrary temperatures $0 \leq T \leq T_c$ the numerical solution of Eq. (D7) is shown in Fig. 17.

-
- [1] M. Sigrist and T.M. Rice, J. Phys. Soc. Japan 61 (1992) 4283; M. Sigrist, Progr. Theor. Phys. 99 (1998) 899.
- [2] V.B. Geshkenbein, A.I. Larkin, and A. Barone, Phys. Rev. B 36 (1987) 235.
- [3] D.A. Wollman, D. J. Van Harlingen, W. C. Lee, D. M. Ginsberg, and A. J. Leggett, Phys. Rev. Lett. 71 (1993) 2134.
- [4] D.J. Van Harlingen, Rev. Mod. Phys. 67 (1995) 515.
- [5] C.C. Tsuei, J.R. Kirtley, M. Rupp, J.Z. Sun, A. Gupta, M.B. Ketchen, C.A. Wang, Z.F. Ren, J.H. Wang, and M. Bhushan, Science 271 (1996) 329.
- [6] V.V. Ryazanov, V. A. Oboznov, A.Yu. Rusanov, A.V. Veretennikov, A. A. Golubov, and J. Aarts, Phys. Rev. Lett. 86 (2001) 2427.
- [7] A. Huck, A. van Otterlo, and M. Sigrist, Phys. Rev. B 56 (1997) 14163.
- [8] A.M. Zagoskin and M. Oshikawa, J. Phys.: Cond. Mat. 10 (1998) L105.
- [9] A.F. Andreev, Zh. Eksp. Teor. Fiz. 46 (1964) 1823.
- [10] A.M. Zagoskin, “Quantum Theory of Many-Body Systems”, Springer-Verlag New York (1998).
- [11] I.O. Kulik, Zh. Eksp. Teor. Fiz. 57 (1969) 1745.
- [12] C. Ishii, Prog. Theor. Phys. 44 (1970) 1525.
- [13] J. Bardeen and J.L. Johnson, Phys. Rev. B 5 (1972) 72.
- [14] A. Furusaki, Superlat. and Microstruct. 25 (1999) No.5/6.
- [15] R.A. Riedel and P.F. Bagwell, Phys. Rev. B 57 (1998) 6084.
- [16] S. Kashiwaya and Y. Tanaka, Rep. Prog. Phys. 63 (2000) 1641.
- [17] T. Löfwander, V.S. Shumeiko, and G. Wendin, Supercond. Sci. Technol. 14 (2001) R53.
- [18] C.R. Hu, Phys. Rev. Lett. 72(1994) 1526.
- [19] S. Yip, J. Low Temp. Phys. 91 (1993) 203.
- [20] Y. Tanaka, Phys. Rev. Lett. 72 (1994) 3871; Y. Tanaka and S. Kashiwaya, Phys. Rev. B 56 (1997) 892.
- [21] A.M. Zagoskin, J. Phys.: Cond. Matter 9 (1997) L419.
- [22] Y. Tanaka and S. Kashiwaya, Phys. Rev. B **53**, 2948 (1996); Yu.S. Barash, H. Burkhardt, and D. Rainer, Phys. Rev. Lett. 77 (1996) 4070.
- [23] E. Il’ichev, M. Grajcar, R. Hlubina, R.P.J. IJsselsteijn, H.E. Hoenig, H.-G. Meyer, A. Golubov, M.H.S. Amin, A.M. Zagoskin, A.N. Omelyanchouk, and M.Yu. Kupriyanov, Phys. Rev. Lett. 86 (2001) 5369.
- [24] M.H.S. Amin, A.N. Omelyanchouk, and A.M. Zagoskin, Phys. Rev. B 63 (2001) 212502.
- [25] I. Iguchi, W. Wang, M. Yamazaki, Y. Tanaka, and S. Kashiwaya, Phys. Rev. B 62 (2000) R6131.
- [26] E.M. Lifshits and L.P. Pitaevskii, “Statistical Physics: Part II”, v.IX, §54, Oxford; New York: Pergamon Press (1980).
- [27] M. Covington, M. Aprili, E. Paraoanu, L.H. Greene, F. Xu, J. Zhu, and C.A. Mirkin, Phys. Rev. Lett. 79 (1997) 277; L.H. Greene, M. Covington, M. Aprili, E. Badica, and D.E. Pugel, Physica B 280 (2000) 159.
- [28] F. Tafuri and J.R. Kirtley, preprint (cond-mat/0003106).
- [29] V. Barzykin and A.M. Zagoskin, Superlat. and Microstruct. 25 (1999) 797.
- [30] A. Zagoskin, cond-mat/9903170; A. Blais and A.M. Zagoskin, Phys. Rev. A 61 (2000) 042308.
- [31] G. Eilenberger, Z. Phys. 214 (1968) 195.
- [32] I.O. Kulik and A.N. Omelyanchouk, Sov. J. Low Temp. Phys. 3, 459 (1977); 4 (1978) 142.
- [33] D.J. Van Harlingen, talk at APS March Meeting (W27.002) (2001).
- [34] D.B. Bailey, M. Sigrist, and R.B. Laughlin, Phys. Rev. B 55 (1997) 15239.
- [35] M. Matsumoto and H. Shiba, J. Phys. Soc. Jap. 64 (1995) 4867.
- [36] A.A. Golubov and M.Yu. Kupriyanov, preprint cond-mat/9803369; Superlatt. and Microstruct., 25 (1999) 949.
- [37] I.F. Herbut, Private communication.
- [38] W.K. Neils and D.J. Van Harlingen, preprint (cond-mat/0105388).
- [39] L.B. Ioffe, V.B. Geshkenbein, M.V. Feigel’man, A.L. Fauchere, and G. Blatter, Nature 398 (1999) 679.
- [40] The self-consistent calculations in tight-binding model [J.J. Hogan-O’Neill, A.M. Martin, and J.F. Annett, Phys. Rev. B 60 (1999) 3568] did not yield \mathcal{T} -breaking in a symmetric 53.1°-junction, which may be the result of the specific model used.
- [41] S. Higashitani, J. Phys. Soc. Jpn. 66 (1997) 2556.
- [42] C. Honerkamp and M. Sigrist, Physica C 317-318 (1999) 489.
- [43] Yu. S. Barash, M. S. Kalenkov, and J. Kurkijärvi, Phys. Rev. B 62 (2000) 6665.
- [44] T. Löfwander, V. S. Shumeiko, and G. Wendin, Phys. Rev. B 62 (2000) R14653.
- [45] Y. Tanaka and S. Kashiwaya, Phys. Rev. B 58 (1998) 2948.
- [46] N. Schopohl and K. Maki, Phys. Rev. B 52 (1995) 490; N. Schopohl, preprint (cond-mat/9804064).
- [47] A.V. Zaitsev, JETP 59 (1984) 1015.
- [48] Yu.S. Barash, A.V. Galaktionov, and A.D. Zaikin, Phys. Rev. B. 52 665 (1995).
- [49] M. Eschrig, Phys. Rev. B **61** (2000) 9061.
- [50] F.J. Gulletto, G. Keiselmann, and D. Rainer, in *Proceedings of the 17th International Conference on Low Temperature Physics* (North Holland, Amsterdam, 1984) p. 1027.
- [51] A.N. Omelyanchouk, R. de Bruyn Ouboter, and C.J. Muller, Low Temp. Phys. 20 (1994) 398.
- [52] A.A. Golubov, and M.Yu. Kupriyanov, JETP Lett. 69 (1999) 262.